Indoor Air 2014; 24: 376–389
wileyonlinelibrary.com/journal/ina

INDOOR AIR
doi:10.1111/ina.12092

Secondary organic aerosol in residences: predicting its fraction of fine particle mass and determinants of formation strength

Abstract Indoor secondary organic aerosol (SOA) formation may contribute to particle concentrations within residences, but little systematic work has investigated its magnitude or the determinants of its formation. This work uses a time-averaged modeling approach to predict the indoor SOA mass formed in residences due to the oxidation of 66 reactive organic compounds by ozone or the hydroxyl radical, parameterizing SOA formation with the aerosol mass fraction. Other organic and inorganic aerosols owing to outdoor and indoor sources were also predicted. Model inputs were represented as distributions within a Monte Carlo analysis, so that result distributions and sensitivity of results to inputs could be quantified, using a dataset developed from the study of Relationships between Indoor, Outdoor and Personal Air and other sources. SOA comprised a large amount of indoor organic and total fine particles for a subset of the results (e.g., >47% of indoor organic and >30% of fine aerosol for 10% of the modeled cases), but was often a small fraction. The sensitivity analysis revealed that SOA formation is driven by high terpene emission rates (particularly by d-limonene) and outdoor ozone, along with low air exchange and ozone and particle deposition rates.

M. S. Waring

Department of Civil, Architectural and Environmental Engineering, Drexel University, Philadelphia, PA, USA

Key words: Indoor SOA; d-Limonene; Ozone; Hydroxyl radical; Aerosol mass fraction; Yield.

M. S. Waring
Department of Civil
Architectural and Environmental Engineering
Drexel University
3141 Chestnut St., Philadelphia
PA 19104
USA
Tel.: 011-215-895-1502
Fax: 011-215-895-1363
e-mail: msw59@drexel.edu

Received for review 9 September 2013. Accepted for publication 24 December 2013.

Practical Implications

This study predicts that indoor SOA formation can be a substantial fraction of indoor aerosols in residences, for certain combinations of building and reactant parameters. The model herein can predict SOA for risk analyses or be used to design experiments to study indoor SOA formation. The terpene, d-limonene, contributes by far the most to formation, and eliminating this particular compound indoors would be impactful on indoor aerosol concentrations.

Introduction

People in developed countries spend nearly 90% of their lives indoors, mostly within residences (e.g., Klepeis et al., 2001), in which they are exposed to air pollutants such as ozone (O_3) (Weschler, 2000), volatile and semivolatile organic compounds (Brown et al., 1994; Weschler and Nazaroff, 2008), and fine particles (Wallace, 2006). Indoor exposures to these pollutants negatively impact human health (e.g., Logue et al., 2011; Weschler, 2006; Weschler and Nazaroff, 2008), and since humans inhabit residences a dominant fraction of the time, reducing residential indoor exposure to any of these contaminants is a worthy goal. As such, this study investigates the residential particle source of secondary organic aerosol (SOA), which forms due to products of oxidative reactions with reactive organic compounds (ROG) indoors.

Given that a large fraction of urban particles is composed of SOA (e.g., Polidori et al., 2006a) and increases in urban particle concentrations have been correlated with observable health impacts (Pope and Dockery, 2006), it is feasible though not certain that exposure to indoor-generated SOA may have health effects (Rohr, 2013). One study, though, found that acute airway effects owing to reactions of O_3 and d-limonene were caused by gaseous not aerosol products, using mouse bioassays (Wolkoff et al., 2008). Furthermore, SOA may negatively influence health by acting as sorptive reservoirs for either reactive oxygen species (ROS) formed during oxidative processes (Chen et al., 2011) or for semivolatile organic compounds (SVOC) emitted indoors, such as plasticizers or pesticides (Benning et al., 2013; Liu et al., 2012; Weschler and Nazaroff, 2008).

Weschler and Shields (1999) first observed SOA formation indoors from reactions of O_3 and d-limonene and other terpenoids, and since then, indoor SOA research has almost solely focused on that which forms because of O_3 gas-phase reactions with terpenoid ROGs (e.g., Chen and Hopke, 2009, 2010; Coleman et al., 2008; Destaillats et al., 2006; Fadeyi et al., 2009, 2013; Sarwar and Corsi, 2007; Sarwar et al., 2003; Wainman et al., 2000; Waring et al., 2008, 2011; Zuraimi et al., 2007), although SOA derived from ozone surface reactions with sorbed d-limonene (Waring and Siegel, 2013) and squalene (Wang and Waring, 2014) has also been studied. Terpenoids are prevalent indoors and emitted by consumer product use (Coleman et al., 2008; Destaillats et al., 2006; Singer et al., 2006a,b). Indoor O_3 sources include outdoor-to-indoor transport (Sabersky et al., 1973) or emissions from office equipment (Lee et al., 2001) and ion or O_3 generators (Britigan et al., 2006; Hubbard et al., 2005; Niu et al., 2001; Tung et al., 2005; Waring et al., 2008).

At typical concentrations in homes, O_3 and ROG reactions likely occur and generate SOA at fast enough rates to influence particle concentrations, yet little is known about the actual magnitude of SOA in residences. Other residential indoor aerosol sources are strong and could dominate SOA formation, including ambient particle infiltration (Riley et al., 2002; El Orch et al., 2014), cooking (Wallace, 2006), or smoking (Wallace, 1996). Nevertheless, the study of the Relationships between Indoor, Outdoor and Personal Air (RIOPA) measured organic and total fine particle concentrations in non-smoking homes in three U.S. cities, and it estimated that 40–75% of the measured organic aerosol was generated indoors and speculated that SOA was a contributor (Polidori et al., 2006b). Moreover, Weschler (2006) noted that data from a field study in Baltimore discussed in Sarnat et al. (2005) supports the role of indoor SOA comprising meaningful fractions of indoor particle mass, due to differences noted in winter and summer months that were attributed to differences in outdoor O_3 formation.

This study explores the contributing fraction of SOA to residential indoor concentrations of organic and fine aerosol mass, as well as the strength of determinants on SOA formation, with a modeling approach. SOA mass formation is predicted with the aerosol mass fraction, AMF or ξ (Hoffmann et al., 1997; Odum et al., 1996), within the 'volatility basis set' (VBS) framework (Donahue et al., 2006; Presto and Donahue, 2006). As indoor studies have investigated SOA mostly from O_3 and terpenoid reactions, this work explores the possible influence of oxidation of 66 ROGs of different chemical classes. Considered determinants include the oxidation of ROGs by O_3 and the hydroxyl radical (OH), as well as building and environmental variables, using a dataset assembled from the RIOPA study but supplemented by other studies for ROGs not measured during that campaign. Input variables were modeled as probability distributions and used in a Monte Carlo approach so that distributions of results could be predicted, as well as so the influence of inputs on SOA formation could be quantified.

Modeling methodology

Overview of model

The model predicts indoor concentrations of the oxidants O_3 and OH; a set of 66 reactive organic gases (ROG *j*); organic and inorganic aerosol components from outdoor sources (OOA and OIA, respectively); organic and inorganic aerosol components emitted by primary indoor sources (POA and PIA, respectively); and indoor-generated SOA. As such, the total indoor organic aerosol mass (OA) is OA = OOA + POA + SOA; the total inorganic aerosol mass (IA) is IA = OIA + PIA; and the total fine particulate matter (PM) mass concentration is PM = OA + IA. To be clear, the OA and IA distinctions do not necessary represent physically distinct aerosol populations, but rather they represent the organic and inorganic amounts within the total aerosol mass concentration.

The RIOPA data used to generate model inputs were indoor and outdoor 48-h samples (Weisel et al., 2005) that measured select ROGs, fine particle mass (i.e., <2.5 μm in diameter), and the organic fraction of those fine particles (as well as air exchange and deposition rates). Therefore, time-averaged (Riley et al., 2002), volume-normalized mass balances were written to predict time-averaged indoor concentrations (with a generic one representing each ROG *j*), which are Equations 1–8. Also, two expressions for predicting SOA mass generation due to oxidation of organic gases by O_3 or OH were written, which are Equations 9 and 10.

Predicting indoor concentrations

The schematic in Figure 1 illustrates the oxidant, ROG *j*, and aerosol fate and transport in the model, and the variables thereon were used in the mass balances and SOA formation expressions. The mass balances for each pollutant assume the indoor air is a single well-mixed control volume with air exchange due to infiltration or open doors and windows, as with homes in the RIOPA study. In Equations 1–8, numerator terms are sources, and denominator terms are losses. Sources may be due to outdoor-to-indoor transport, as with O_3, OH, the ROGs, OOA and OIA, or they may be due to indoor emission or generation, as with OH, the ROGs, POA, SOA, and PIA. All species are reduced by air exchange. Other O_3 and OH losses are surface and gas-phase reactions; another ROG loss is gas-

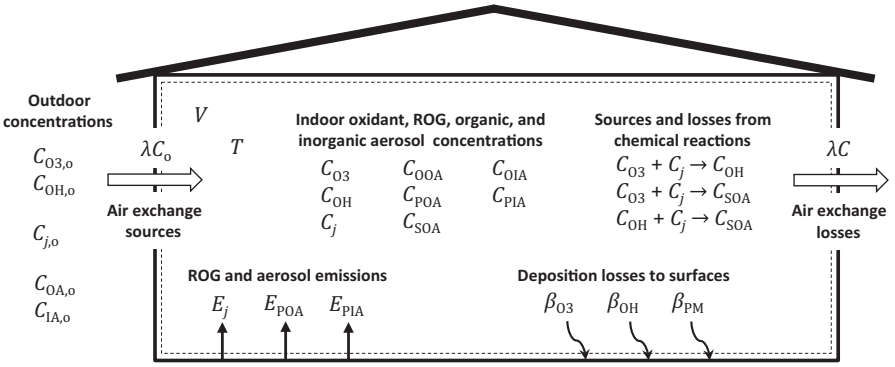

Fig. 1 Schematic for accounting for ozone, hydroxyl radical, reactive organic gas (ROG *j*), and aerosol fate and transport in the residential indoor air SOA formation model. See text for variable definitions and model equations

phase reactions; and another loss for all aerosols is total deposition, which may include the deposition to indoor surfaces or onto filters in a recirculating air system. Attenuation of O_3, OH, OOA, and OIA owing to losses within the envelope with infiltration air is neglected as some air exchange is through large openings. Sorption of ROGs to indoor material surfaces is dynamic and thus not included.

Equations 1–3 are the mass balances for gases. The indoor O_3 mole fraction, C_{O3} (ppb), is:

$$C_{O3} = \frac{\lambda C_{O3,o}}{\lambda + \beta_{O3} + \sum_j (k_{j(O3)} C_j)} \tag{1}$$

where λ (h^{-1}) is the air exchange rate; β_{O3} (h^{-1}) is the O_3 surface deposition rate; $C_{O3,o}$ (ppb) is the outdoor O_3 mole fraction; C_j (ppb) is the indoor ROG *j* mole fraction; and $k_{j(O3)}$ (ppb^{-1} h^{-1}) is the bimolecular reaction rate constant for O_3 and ROG *j*. Reactions of O_3 and unsaturated ROGs (e.g., terpenes, alkenes) yield OH indoors (e.g., Weschler and Shields, 1996), and the indoor OH mole fraction, C_{OH} (ppb), is:

$$C_{OH} = \frac{\lambda C_{OH,o} + C_{O3} \sum_j (Y_{OH,j(O3)} k_{j(O3)} C_j)}{\lambda + \beta_{OH} + \sum_j (k_{j(OH)} C_j)} \tag{2}$$

where β_{OH} (h^{-1}) is the surface deposition rate of OH; $C_{OH,o}$ (ppb) is the outdoor OH mole fraction; $k_{j(OH)}$ (ppb^{-1} h^{-1}) is the bimolecular reaction rate constant for OH and ROG *j*; and $Y_{OH,j(O3)}$ is the molar yield of OH resulting from O_3 reactions with any unsaturated ROG *j*. The indoor mole fraction for any ROG *j*, C_j (ppb), is:

$$C_j = \frac{\lambda C_{j,o} + E_j/V}{\lambda + k_{j(O3)} C_{O3} + k_{j(OH)} C_{OH}} \tag{3}$$

where $C_{j,o}$ (ppb) is the outdoor concentration of ROG *j*; and E_j/V (ppb/h) is the volume-normalized emission rate of ROG *j* from all indoor sources (i.e., a 'whole-house' emission rate). The oxidation of ROGs by any other oxidant (e.g., nitrate radicals) is neglected.

Equations 4–6 are mass balances for organic aerosol mass concentrations. The indoor concentration of the OOA from outdoor-to-indoor transport, C_{OOA} ($\mu g/m^3$), is:

$$C_{OOA} = \frac{\lambda C_{OA,o}}{\lambda + \beta_{PM}} \tag{4}$$

where $C_{OA,o}$ ($\mu g/m^3$) is the outdoor organic aerosol concentration; and β_{PM} (h^{-1}) is the total deposition rate of all PM types in the model. Although different types of PM may have different deposition rates indoors, this study used one value for all aerosol components due to uncertainty in individual loss rates. The indoor-generated POA concentration, C_{POA} ($\mu g/m^3$), is:

$$C_{POA} = \frac{E_{POA}/V}{\lambda + \beta_{PM}} \tag{5}$$

where E_{POA}/V ($\mu g/m^3$ h) is the volume-normalized emission rate of POA from all combined indoor sources. Equations 4 and 5 assume that any so-called OOA and POA indoors are composed of non-volatile elements and no mass is lost due to semivolatile repartitioning, as there is not sufficient information to predict the volatility distributions of those aerosols. The SOA formed indoors owing to ROG *j* oxidation by O_3 or OH, C_{SOA} ($\mu g/m^3$), is:

$$C_{SOA} = \frac{C_{O3} \sum_j (\xi_{j(O3)} k_{j(O3)} C_j \Gamma_J) + C_{OH} \sum_j (\xi_{j(OH)} k_{j(OH)} C_j \Gamma_J)}{\lambda + \beta_{PM}} \tag{6}$$

where $\xi_{j(O3)}$ and $\xi_{j(OH)}$ are the AMFs for ROG *j* oxidation by O_3 or OH, respectively; and Γ_j is a temperature-dependent conversion factor to change units from ppb to $\mu g/m^3$ for ROG *j*.

Equation 6 is similar to the SOA formation model in Youssefi and Waring (2012) for single terpenoid ozonolysis, but it has been expanded to include SOA formation due to multiple ROGs and OH oxidation as well. Odum et al. (1996, 1997) demonstrated that SOA formation resulting from the oxidation of a mixture of ROGs could be predicted as the summed formation predicted by the AMFs for the individual parent compounds, so Equation 6 should be appropriate to use indoors. To determine C_{OA} ($\mu g/m^3$), the total indoor organic aerosol concentration, one uses $C_{OA} = C_{OOA} + C_{POA} + C_{SOA}$.

Equations 7 and 8 are mass balances for inorganic aerosol mass concentrations from different sources, and the inorganic aerosol components of OIA and PIA were determined with mass balances and assumptions similar to OOA and POA, respectively. The indoor concentration of OIA due to outdoor-to-indoor transport, C_{OIA} ($\mu g/m^3$), is:

$$C_{OIA} = \frac{\lambda C_{IA,o}}{\lambda + \beta_{PM}} \tag{7}$$

where $C_{IA,o}$ ($\mu g/m^3$) is the outdoor inorganic aerosol concentration. The indoor-generated PIA concentration, C_{PIA} ($\mu g/m^3$), is:

$$C_{PIA} = \frac{E_{PIA}/V}{\lambda + \beta_{PM}} \tag{8}$$

where E_{PIA}/V ($\mu g/m^3$ h) is the volume-normalized emission rate of PIA from all indoor sources. To find C_{IA} ($\mu g/m^3$), the total indoor inorganic aerosol concentration, one uses $C_{IA} = C_{OIA} + C_{PIA}$. Furthermore, the total fine particle concentration indoors, C_{PM} ($\mu g/m^3$), is $C_{PM} = C_{OA} + C_{IA}$.

This indoor SOA formation model describes the overall partitioning behavior of ROG j oxidation products with the aerosol mass fraction (also called the SOA yield) for ROG j by either oxidant (ox) O_3 or OH, which is the ratio of the mass of organic aerosol formed, ΔC_{SOA} ($\mu g/m^3$), to the mass of ROG j reacted, ΔC_j ($\mu g/m^3$), as in Equation 9:

$$\xi_{j(ox)} = \frac{\Delta C_{SOA}}{\Delta C_j} = \sum_i \left(\frac{\alpha_{i(ox)}}{1 + (c_i^*/C_{OA})} \right) = \sum_i \left(\frac{\alpha_{i(ox)}}{1 + (c_i^*/(C_{SOA} + C_{POA} + C_{OOA}))} \right) \tag{9}$$

where the $\xi_{j(ox)}$ is the AMF for ROG j oxidation by O_3 or OH as represented by a multiproduct model; $\alpha_{i(ox)}$ is the mass-based yield of product i for either oxidant (ox); and c_i^* ($\mu g/m^3$) is the effective gas-phase saturation concentration of species or group i (Odum et al., 1996; Presto and Donahue, 2006). A multiproduct model describes SOA formation by lumping contributions of products with similar volatilities. Rather than the Odum one- or two-product model, this study uses the 'volatility basis set' (VBS) approach, which is more effective at the lower C_{OA} (i.e., <10 $\mu g/m^3$) typical of many indoor settings. Also, the two-product model is problematic because its parameters are not orthogonal and have high covariance (Presto and Donahue, 2006). The VBS overcomes this shortcoming by constraining the c_i^* at logarithmically spaced intervals and describing formation results with fits of α_i at those c_i^*. As shown in Equation 9, as the C_{OA} increases (i.e., from OOA, POA, or SOA), so does the AMF.

AMFs determined from laboratory experiments are usually reported as normalized to a particle density of 1 g/cm^3 and a reference temperature of 298 K so that variations in density and temperature can easily be modeled. To convert to values for different cases, the ξ_j is multiplied by the OA density, and the c_i^* may be shifted to reflect the different temperature, $c_i^*(T)$, with the Clausius–Clapeyron equation:

$$c_i^*(T) = c_i^*(T_{298K}) \frac{T_{298K}}{T} \exp\left(\frac{\Delta H_i}{R} \left(\frac{1}{T_{298K}} - \frac{1}{T} \right) \right) \tag{10}$$

where $c_i^*(T_{298K})$ is the c_i^* at the 298 K reference temperature; ΔH_i (kJ/mol) is the enthalpy of evaporation for product i; and R (kJ/K·mol) is the gas constant. Also, the effects of UV light and NO_x on the AMFs for some ROGs have been determined, but these are herein neglected because UV effects are less important indoors than outdoors and NO_x was not measured during the RIOPA campaign, respectively.

Model inputs

Input parameters were taken from the RIOPA set, and when not available, they were drawn from other studies. Probability distributions were used for most of the building and environmental input parameters, including $\{\lambda, T, \beta_{O3}, \beta_{PM}, C_{O3,o}, C_{OA,o}, C_{IA,o}, C_{j,o}, E_{POA}/V, E_{PIA}/V, E_j/V\}$. Single values were used for the variables $C_{OH,o} = 2 \times 10^{-4}$ ppb and $\beta_{OH} = 7.06\ h^{-1}$ (Weschler and Shields, 1996), as indoor OH is chiefly due to indoor OH formation and OH surface reaction rates are uncertain. The distributions used in the Monte Carlo operation were lognormal, except for T, which was normal. Input distribution parameters are listed in Table 1, except for the 66 ROG inputs, which are listed in Table 2. These distributions were directly reported in the literature or were estimated with summary data, and references used for inputs are listed in Tables 1 and 2. Volume-normalized emission rate distributions were calculated in a separate Monte Carlo procedure prior to the primary Monte Carlo analysis, using the distributions for reported indoor and outdoor concentrations and other relevant parameters.

Table 1 Input parameters for Monte Carlo analysis exploring time-averaged SOA formation owing to oxidation of 66 reactive organic gases (ROGs), including the geometric mean (GM) and geometric standard deviation (GSD) for the lognormal distributions and the arithmetic mean (AM) and arithmetic standard deviation (SD) for the normal distribution

Parameter	GM	GSD	1st Percentile	99th Percentile	Source
λ (h^{-1})	0.75	2.1	0.135	4.14	1
β_{O3} (h^{-1})	2.5	1.5	1.08	6.36	2, 3, 4
β_{PM} (h^{-1})	0.79	1.35	0.395	1.57	1
$C_{O3,o}$ (ppb)	25.5	2.04	4.91	108	5
$C_{OA,o}$ ($\mu g/m^3$)	4.02	1.65	1.53	12.6	1, 6
$C_{IA,o}$ ($\mu g/m^3$)	11.5	1.65	4.36	36.6	1, 6
E_{POA}/V ($\mu g/m^3$ h)	7.0	1.75	1.88	26.1	1, 6
E_{PIA}/V ($\mu g/m^3$ h)	2.2	1.75	0.611	8.06	1, 6
$C_{j,o}$ (ppb)	Table 2 for 66 ROG j				1, 7, 8
E_j/V (ppb/h)	Table 2 for 66 ROG j				1, 7, 8
	AM	SD			
T (K)	296.9	3.0	290	302	1

1. Weisel et al. (2005).
2. Lee et al. (1999).
3. USEPA (2006).
4. Morrison et al. (2011).
5. Youssefi and Waring (2012).
6. Turpin et al. (2007).
7. Weschler and Shields (1996).
8. Sarwar et al. (2002).

In the RIOPA study, 29 ROGs were measured, consisting primarily of monoterpenes, aromatics, carbonyls, and chlorinated compounds. For most carbonyls in the RIOPA study, active and passive methods were used for sample collection, and in that case, this work used the average of the two results. As a major objective of this study was to examine the relative influence on indoor SOA production of the oxidation of different ROGs, this dataset was supplemented to include more ROGs typically found in residences, from Weschler and Shields (1996) and Sarwar et al. (2002). From these, 37 more compounds were included, mostly comprising additional monoterpenes, alkenes, alcohols, and alkanes. For these other studies, distribution data were not available, so distribution characteristics were assumed that mimicked those for similar compounds in the RIOPA study. Thus, the input dataset was not meant to perfectly represent the RIOPA set; rather, the RIOPA and other data were used to construct a realistic, reasonable modeling space in which the study questions could be explored.

These parameters, $\{k_{j(O3)}, k_{j(OH)}, Y_{OH,j(O3)}, \xi_{j(O3)}, \xi_{j(OH)}\}$, relate to the oxidation of the 66 ROGs. For the oxidation by O_3 or OH of the 66 ROGs, temperature-dependent rate constants, $k_{j(O3)}$ and $k_{j(OH)}$, were taken from the Master Chemical Mechanism, MCM v3.2 (Bloss et al., 2005; Jenkin et al., 1997, 2003; Saunders et al., 2003). Of the 66 ROGs, nine rate constants were not part of the MCM, so these were either taken from other sources or assumed as the same as the most similar compound. Table 2 lists the rate constants at the mean temperature (AM = 296.9 K) for all ROGs, as well as references for the nine rates not in the MCM. The OH molar yields for relevant O_3/ROG j reactions, $Y_{OH,j(O3)}$, were from Weschler and Shields (1996), and those are listed in Table 2 as well.

To facilitate SOA formation modeling and subsequent analysis, the 66 ROGs were lumped into 13 SOA-forming groups according to the grouping used in Lane et al. (2008). The 13 groups and their VBS parameters for their AMFs, $\xi_{j(O3)}$ and $\xi_{j(OH)}$, are in Table 3. There are six monoterpenes, which are considered individually due to their high formation potential, and they are d-limonene (DLIM), α-pinene (APIN), β-pinene (BPIN), camphene (CAMP), α-terpinene (ATERP), and Δ3-carene (D3CAR). The remaining ROG groups are two lumped olefin groups (OLE1 and OLE2), isoprene (ISO), two aromatic groups (ARO1 and ARO2), and two high molecular weight alkane groups (ALK4 and ALK5).

This work uses AMFs represented by the VBS model with a four-product basis set over c_i^* (T_{298K}) spaced at 1, 10, 100, and 1000 $\mu g/m^3$, as listed in Table 3. The AMFs for all ROGs except the terpenes were from the base case in Lane et al. (2008). The AMFs for d-limonene and α-pinene were from experiments without UV or NO_x in Zhang et al. (2006) and Presto and Donahue (2006), respectively. For the other terpenes, the AMFs were estimated by scaling two-product AMFs to the VBS AMF of α-pinene. The initial two-product fits for β-pinene, α-terpinene, and Δ3-carene were those reported in Griffin et al. (1999); camphene was assumed as the same as β-pinene as both have similar exocyclic double bonds. When AMFs from ozonolysis and photooxidation experiments were available, one AMF was determined as an average weighted by O_3 and OH reactivity for the compound (assuming the median resulting indoor O_3 and OH mole fractions). For simulated cases at different temperatures, the c_i^* (T_{298K}) was adjusted to the relevant temperature using ΔH_i = 30 kJ/mol (Lane et al., 2008). The density of SOA was assumed as 1.6 g/cm^3 (Chen and Hopke, 2009).

Solution procedure

The Monte Carlo operation used input values that were randomly sampled from the input probability distributions to solve for 10 000 unique cases the time-averaged indoor concentrations of $\{C_{O3}, C_{OH}$, the 66 C_j, $C_{SOA}, C_{OOA}, C_{POA}, C_{OA}, C_{OIA}, C_{PIA}, C_{IA}, C_{PM}\}$. For each case, the simultaneous solution of the model equations was required. The solution procedure recognizes that time-averaged and steady state equations to predict indoor concentrations are identical in form (Riley et al., 2002). Therefore, to solve the model equations simultaneously, Equations 1–8 were cast into their differential form and solved simultaneously with

Table 2 Summary of model inputs and outputs for 66 considered reactive organic gases (ROG *j*)

Compound[1]	$k_{j(O3)}$[2] (ppb^{-1} h^{-1})	$k_{j(OH)}$[2] (ppb^{-1} h^{-1})	Y_{OH}[3] (—)	$\xi_{j(O3)}$[4] (—)	$\xi_{j(OH)}$[4] (—)	E_j/V^5 (ppb/h) GM (GSD)	$C_{j,o}$[6] (ppb) GM (GSD)	C_j[7] (ppb) GM (GSD)
Terpenes								
d-Limonene (a)	1.9E−02	1.5E+04	0.86	DLIM	DLIM	1.5 (4.8)	0.23 (2.5)	2.2 (3.8)
α-Pinene (a)	7.9E−03	4.7E+03	0.85	APIN	APIN	0.23 (6.7)	0.057 (2.7)	0.43 (4.3)
β-Pinene (a)	1.3E−03	7.0E+03	0.35	BPIN	BPIN	0.19 (5.4)	0.032 (1.3)	0.32 (4.1)
Camphene (b)	7.9E−03	4.7E+03	0.15	CAMP	CAMP	0.22 (5.6)	0.083 (1.8)	0.43 (3.5)
α-Terpinene (b)	7.5E−01	3.2E+04	0.91	ATERP	ATERP	0.15 (5.5)	0.010 (1.8)	0.035 (5.2)
Δ3-carene (c)	3.3E−03	7.8E+03	0.85	D3CAR	D3CAR	0.17 (5.5)	0.020 (1.8)	0.26 (4.3)
Alkenes								
Ethene (b)	1.4E−04	7.6E+02	0.12	–	–	0.72 (3.8)	0.50 (1.3)	1.7 (2.4)
Propene (b)	8.7E−04	2.3E+03	0.33	–	–	0.24 (3.8)	0.16 (1.3)	0.56 (2.5)
trans-2-Butene (b)	1.7E−02	5.7E+03	0.64	–	OLE1	0.13 (3.7)	0.073 (1.3)	0.25 (2.5)
cis-2-Butene (b)	1.1E−02	5.0E+03	0.41	–	OLE1	0.14 (3.7)	0.080 (1.3)	0.27 (2.5)
Isobutene (b)	9.9E−04	4.6E+03	0.84	–	OLE2	0.24 (3.8)	0.16 (1.3)	0.56 (2.5)
1,3-Butadiene (b)	5.5E−04	6.0E+03	0.08	OLE1	OLE2	0.15 (3.7)	0.10 (1.3)	0.35 (2.4)
2-Methyl-2-butene (b)	3.6E−02	7.8E+03	0.89	OLE1	OLE2	0.16 (3.5)	0.077 (1.3)	0.26 (2.7)
Styrene (a)	1.5E−03	5.2E+03	0.37	OLE2	OLE2	0.059 (3.8)	0.040 (1.3)	0.14 (2.5)
Isoprene (b)	1.1E−03	8.9E+03	0.27	ISOP	ISOP	1.0 (3.8)	0.67 (1.3)	2.3 (2.5)
Aromatics								
Benzene (a)	–	1.1E+02	–	–	ARO1	0.35 (4.6)	0.53 (2.0)	1.3 (2.4)
Toluene (a)	–	5.0E+02	–	–	ARO1	1.2 (4.2)	1.4 (1.5)	3.6 (2.3)
Phenol (c)	–	9.8E+02	–	–	ARO2	1.2 (4.2)	0.80 (2.1)	3.1 (2.8)
m- and p-Xylenes (a)	–	1.6E+03	–	–	ARO2	0.62 (4.8)	0.57 (2.4)	1.8 (2.8)
o-Xylene (a)	–	1.2E+03	–	–	ARO2	0.19 (4.5)	0.22 (2.2)	0.59 (2.5)
Ethylbenzene (a)	–	6.2E+02	–	–	ARO2	0.17 (4.5)	0.21 (2.0)	0.57 (2.5)
Isopropyl benzene (c)	–	5.6E+02	–	–	ARO2	0.10 (4.2)	0.060 (2.1)	0.24 (2.8)
1,2,4-Trimethylbenzene (b)	–	2.9E+03	–	–	ARO2	1.1 (4.6)	1.7 (2.1)	3.9 (2.3)
1,3,5-Trimethylbenzene (b)	–	5.0E+03	–	–	ARO2	0.54 (4.4)	0.83 (2.1)	1.9 (2.4)
p-Dichlorobenzene (a)	–	3.8E+01	–	–	ARO2	0.14 (4.5)	0.12 (2.4)	0.39 (2.8)
Aldehydes, ketones, alcohols, and ethers								
Formaldehyde (a)	–	7.6E+02	–	–	–	9.6 (2.8)	3.9 (1.7)	18 (2.5)
Acetaldehyde (a)	–	1.3E+03	–	–	–	4.0 (3.9)	2.3 (1.9)	9.1 (2.7)
Propionaldehyde (a)	–	1.7E+03	–	–	–	0.29 (3.6)	0.47 (1.9)	1.0 (2.1)
Acrolein (a)	–	1.8E+03	–	–	–	0.21 (5.3)	0.21 (3.1)	0.70 (3.0)
Butyraldehyde (a)	–	2.1E+03	–	–	–	0.14 (3.9)	0.28 (1.5)	0.55 (2.0)
Crotonaldehyde (a)	1.4E−04	3.0E+03	0.2	OLE1	OLE2	0.10 (4.8)	0.091 (2.3)	0.31 (2.7)
Valeraldehyde (a)	–	2.6E+03	–	–	ALK4	0.25 (3.9)	0.18 (1.9)	0.62 (2.5)
Isovaleraldehyde (a)	–	2.6E+03	–	–	ALK4	0.13 (3.7)	0.11 (2.4)	0.36 (2.6)
Hexaldehyde (a)	–	2.5E+03	–	–	ALK4	0.35 (3.6)	0.50 (1.7)	1.1 (2.1)
Benzaldehyde (a)	–	1.1E+03	–	–	ARO1	0.20 (4.1)	0.45 (1.9)	0.85 (2.1)
Glyoxal (a)	–	1.0E+03	–	–	–	0.20 (3.6)	0.48 (1.5)	0.88 (1.8)
Methylglyoxal (a)	–	1.5E+03	–	–	–	0.24 (3.8)	0.40 (1.6)	0.87 (2.1)
Acetone (a)	–	1.2E+03	–	–	–	1.3 (4.9)	1.2 (2.6)	3.8 (2.8)
Methyl ethyl ketone (c)	–	9.9E+01	–	–	–	5.1 (3.8)	2.3 (2.4)	11 (2.8)
Methanol (b)	–	7.9E+01	–	–	–	5.3 (4.1)	3.3 (2.4)	13 (2.7)
Ethanol (b)	–	2.9E+02	–	–	–	52 (4.1)	33 (2.4)	130 (2.8)
2-Propanol (c)	–	4.5E+02	–	–	–	1.2 (4.1)	0.76 (2.4)	3.0 (2.8)
2-Butoxyethanol (c)	–	2.1E+03	–	–	–	0.10 (4.1)	0.070 (2.4)	0.26 (2.7)
Methyl tert-butyl ether (a)	–	5.1E+01	–	–	–	1.3 (5.2)	1.5 (2.5)	4.2 (2.7)
Alkanes and chlorinated derivatives								
Methane (d)	–	5.6E−01	–	–	–	0	2000	2000 (1.0)
Ethane (b)	–	2.1E+01	–	–	–	1.3 (4.1)	0.83 (2.0)	3.2 (2.7)
Propane (b)	–	9.4E+01	–	–	–	0.80 (4.1)	0.50 (2.0)	2.0 (2.7)
n-Butane (b)	–	2.1E+02	–	–	–	2.1 (4.0)	1.3 (2.0)	5.1 (2.7)
n-Pentane (b)	–	3.5E+02	–	–	ALK4	1.1 (4.0)	0.67 (2.0)	2.6 (2.7)
n-Hexane (c)	–	4.8E+02	–	–	ALK4	0.37 (4.1)	0.23 (2.0)	0.91 (2.6)
n-Heptane (c)	–	6.2E+02	–	–	ALK5	0.16 (4.1)	0.10 (2.0)	0.39 (2.7)
n-Octane (c)	–	7.7E+02	–	–	ALK5	0.48 (4.1)	0.30 (2.0)	1.2 (2.7)
n-Nonane (c)	–	8.9E+02	–	–	ALK5	0.64 (4.1)	0.40 (2.0)	1.6 (2.7)
n-Decane (c)	–	1.0E+03	–	–	ALK5	0.42 (4.1)	0.27 (2.0)	1.0 (2.7)
n-Undecane (b)	–	1.1E+03	–	–	ALK5	0.53 (4.0)	0.33 (2.0)	1.3 (2.7)
n-Dodecane (c)	–	1.2E+03	–	–	ALK5	0.42 (4.1)	0.27 (2.0)	1.0 (2.7)
n-Tridecane (c)	–	1.2E+03	–	–	ALK5	0.81 (4.2)	0.50 (2.0)	2.0 (2.7)

Table 2 Continued

Compound[1]	$k_{j(O3)}$[2] (ppb^{-1} h^{-1})	$k_{j(OH)}$[2] (ppb^{-1} h^{-1})	Y_{OH}[3] (–)	$\xi_{j(O3)}$[4] (–)	$\xi_{j(OH)}$[4] (–)	E_j/V[5] (ppb/h) GM (GSD)	$C_{j,o}$[6] (ppb) GM (GSD)	C_j[7] (ppb) GM (GSD)
n-Tetradecane (c)	–	1.2E+03	–	–	ALK5	0.43 (4.0)	0.27 (2.0)	1.0 (2.7)
n-Pentadecane (c)	–	1.2E+03	–	–	ALK5	0.11 (4.1)	0.067 (2.0)	0.26 (2.7)
Cyclohexane (c)	–	6.4E+02	–	–	–	0.75 (4.0)	0.47 (2.0)	1.8 (2.7)
Methylene chloride (a)	–	4.8E+01	–	–	–	0.21 (5.5)	0.24 (1.9)	0.69 (2.7)
Chloroform (a)	–	1.4E+01	–	–	–	0.12 (4.6)	0.035 (1.5)	0.22 (3.3)
Carbon tetrachloride (a)	–	3.9E−02	–	–	–	0.020 (4.1)	0.10 (1.3)	0.15 (1.6)
1,1,1-Trichloroethane (b)	–	8.2E−01	–	–	–	5.3 (4.1)	3.3 (2.0)	13 (2.7)
Trichloroethylene (a)	–	1.8E+02	–	–	–	0.0068 (4.1)	0.022 (1.7)	0.038 (1.9)
Tetrachloroethylene (a)	–	1.4E+01	–	–	–	0.048 (4.5)	0.083 (2.7)	0.20 (2.5)

1. ROG distributions were derived from (a) the RIOPA dataset (Turpin et al., 2007; Weisel et al., 2005); (b) Weschler and Shields (1996); (c) compounds from Sarwar et al. (2002); or (d) assumed.
2. Temperature-dependent reaction rate constants were from Master Chemical Mechanism, MCM v3.2 (Bloss et al., 2005; Jenkin et al., 1997, 2003; Saunders et al., 2003), except those for phenol (Wu et al., 2012), p-dichlorobenzene (Arnts et al., 1989), glyoxal and methylglyoxal (Plum et al., 1983), acetone (Gierczak et al., 2003), and carbon tetrachloride (Cupitt, 1987). The alkanes n-tridecane, n-tetradecane, and n-pentadecane were assumed as the same as n-dodecane. Reaction rate constants are for the mean temperature of 296.9 K.
3. Weschler and Shields (1996).
4. Aerosol mass fractions (AMF), Zhang et al. (2006), Presto and Donahue (2006), Lane et al. (2008), Griffin et al. (1999). See Table 3 for AMF parameters.
5. Input emission rate distributions were calculated with a separate Monte Carlo prior to the primary one, using indoor and outdoor concentration distributions of ROGs from Weisel et al. (2005), Weschler and Shields (1996), and Sarwar et al. (2002), along with other relevant input distributions.
6. Input outdoor ROG mole fractions from Weisel et al. (2005), Weschler and Shields (1996), and Sarwar et al. (2002)
7. Resulting indoor ROG mole fraction distributions from the primary Monte Carlo analysis.

Table 3 SOA normalized aerosol mass fractions (AMF) for different reactive organic gas (ROG) species and classes (see text) using the 'volatility basis set' approach with a four-product basis set with saturation concentrations at 298 K, c_i^* (T_{298K}), of 1, 10, 100, and 1000 $\mu g/m^3$.

ROG class AMF		c_i^* (T_{298K}) ($\mu g/m^3$)			
No.	Name	1	10	100	1000
1	DLIM	0.32	0.31	0.30	0.60
2	APIN	0.055	0.090	0.12	0.18
3	BPIN	0.044	0.072	0.12	0.22
4	CAMP	0.032	0.052	0.12	0.20
5	ATERP	0.045	0.073	0.12	0.21
6	D3CAR	0.040	0.066	0.10	0.16
7	OLE1	0.001	0.002	0.012	0.045
8	OLE2	0.003	0.006	0.023	0.076
9	ISOP	0.006	0.02	0.01	0
10	ARO1	0.01	0.03	0.075	0.25
11	ARO2	0.02	0.04	0.08	0.25
12	ALK4	0	0.01	0	0
13	ALK5	0	0.1	0	0

the Runge–Kutta order 4 (RK4) method for each of the 10 000 cases until the steady state was reached; the steady state concentrations were then taken as the time-averaged concentrations. The numerical solution was performed with an in-house program written in the statistical programming software Stata version 11 (StataCorp LP, College Station, TX, USA).

Results and discussion

Summary of model results

The resulting oxidant mole fractions distributions were lognormal and are listed in Table 4. These are quite reasonable concentrations. For example, indoor O_3 mole fractions in 143 residences in southern California had an AM ± SD of 13 ± 12 ppb (Avol et al., 1998). Indoor OH has not been measured in residences to my knowledge, but it has been predicted to have an average value of 6.7×10^{-6} ppb in a typical indoor space (Weschler and Shields, 1996). Moreover, Weschler and Shields (1997) inferred an OH concentration of 2.8×10^{-5} ppb in an office with supplementary O_3 and d-limonene. For the 66 ROGs, Table 2 lists the GM and GSD for the resulting indoor mole fraction distributions. The GMs for these ROGs are very similar to the median mole fractions of ROGs reported in the studies from which these inputs were derived, which is expected as those mole fractions were used to derive the E_j/V from which indoor ROG mole fractions were predicted with Equation 3.

Table 4 Summary of result distributions for ozone, hydroxyl radical, and all aerosol types considered in the Monte Carlo analysis, including the geometric mean (GM) and geometric standard deviation (GSD) for lognormal distribution fits and their 1st and 99th percentiles

Parameter	GM	GSD	1st Percentile	99th Percentile
C_{O3} (ppb)	5.0	2.7	0.38	39
C_{OH} (ppb)	2.0×10^{-6}	2.7	1.8×10^{-7}	1.8×10^{-5}
C_{SOA} ($\mu g/m^3$)	1.0	3.8	0.065	27
C_{POA} ($\mu g/m^3$)	4.2	2.0	0.79	21
C_{OOA} ($\mu g/m^3$)	1.8	1.9	0.37	7.2
C_{OA} ($\mu g/m^3$)	8.7	1.7	3.0	38
C_{OIA} ($\mu g/m^3$)	5.3	1.9	1.1	21
C_{PIA} ($\mu g/m^3$)	1.3	2.0	0.26	6.3
C_{IA} ($\mu g/m^3$)	7.2	1.6	2.4	22
C_{PM} ($\mu g/m^3$)	17	1.5	7.4	47

Figure 2a displays box plots of different indoor aerosol concentrations, with organic aerosol components (SOA + OOA + POA = OA) in white, inorganic aerosol (IA) in light gray, and fine aerosol (PM = OA +

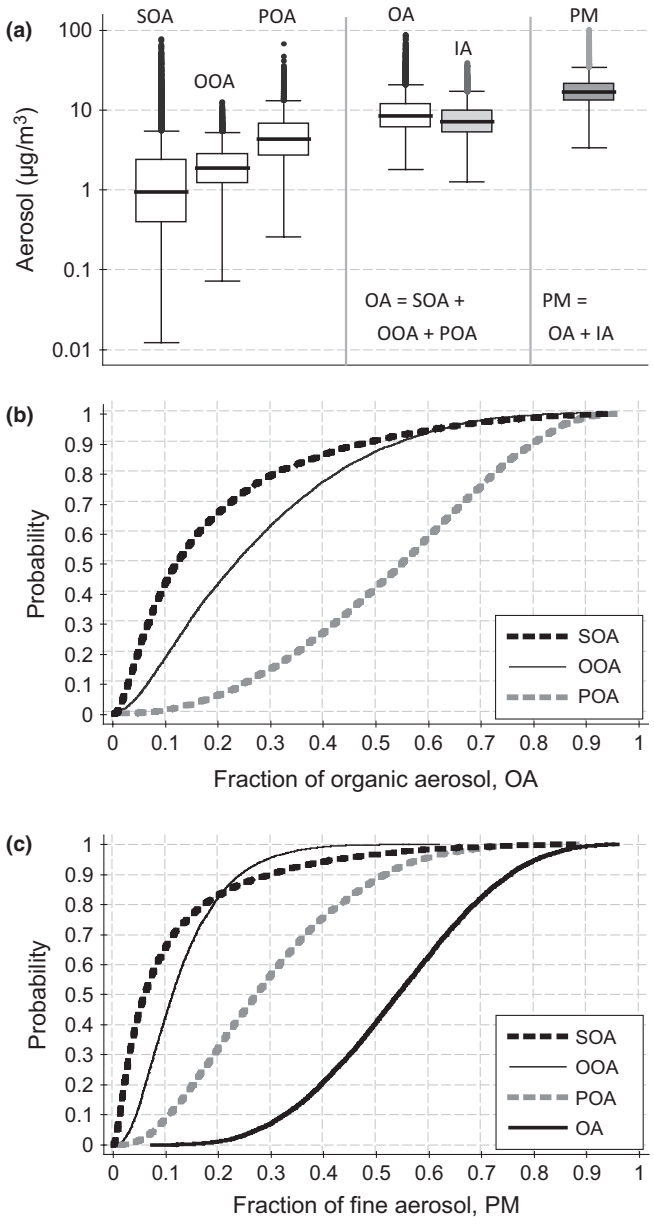

Fig. 2 Results for indoor aerosol generated indoors as secondary organic aerosol (SOA); of outdoor origin (OOA); emitted indoors due to primary emissions (POA); total organic aerosol (OA); inorganic aerosol (IA); and total fine aerosol (PM). Plot (a) is box plots of distributions; and plots (b) and (c) are cumulative distribution functions of the fractions of different organic aerosol types of the indoor (b) total OA and (c) total PM concentrations

IA) in darker gray. The resulting aerosol distributions were also lognormal and summary information for them is listed in Table 4. It was impossible to compare the predicted SOA with the actual measured SOA, as the RIOPA study reported the total OA only. However, the OA and PM distributions are similar to the organic mass and $PM_{2.5}$ distributions from the RIOPA study (Turpin et al., 2007; Weisel et al., 2005), which, for instance, had median values of 7.3 and 14.4 $\mu g/m^3$, respectively. This agreement is sufficient for this work, which uses this dataset to explore the relative magnitudes of SOA as compared to other aerosols and the determinants of the strength of SOA formation.

Relative influence of SOA on indoor aerosols

To illustrate the contribution of the different types of organic aerosol to the total OA concentration, Figure 2b shows cumulative distribution functions (CDF) for ratios of SOA, OOA, and POA to the total OA concentration, over the Monte Carlo set. The SOA comprises the smallest fraction of OA, followed by OOA, and then finally, the POA constitutes the largest fraction. For instance, the fraction of the SOA/OA is 0.056, 0.12, and 0.26 at the 25th, 50th, and 75th percentiles, respectively. In contrast, at those same percentiles, the OOA/OA is 0.13, 0.24, and 0.39, and the POA/OA is 0.39, 0.55, and 0.70, respectively. Moreover, Figure 2b illustrates that for 10% of all modeled cases, the indoor-formed SOA is at least a factor of 0.47 of all OA indoors. It thus appears that indoor SOA formation is only meaningful for certain combinations of parameters (i.e., reactants, building, and environmental factors) within this modeling set. The parameters that have strong impacts on SOA formation are explored in the sensitivity analysis later.

Figure 2c shows CDFs for ratios of SOA, OOA, POA, and OA to the fine aerosol (PM) concentration calculated over the Monte Carlo set. The specific fraction of organic aerosol types to the total indoor PM concentration depends on the relative strengths of the various ambient and indoor particle sources. The OA/PM ratio is 0.42, 0.54, and 0.66 at the 25th, 50th, and 75th percentiles, respectively, thus illustrating the strong presence of organic aerosol in indoor fine particles. This is expected, as in the RIOPA study, most of the $PM_{2.5}$ that was generated indoors was organic aerosol in nature (Polidori et al., 2006b). The trend for the fraction of the different types of organic aerosol to indoor $PM_{2.5}$ follows a similar trend to the fraction of each type to OA, but with lower values. The fraction of SOA/PM is 0.026, 0.060, and 0.14 at the 25th, 50th, and 75th percentiles, respectively. Similar to the SOA/OA fraction, the SOA is only a substantial fraction of indoor fine aerosol for certain combinations of model inputs.

Relative contribution of oxidation of ROGs to indoor SOA

The contributions of each of the 66 ROGs were quantified according to the 13 compound groupings used to assign the AMFs for the oxidation by O_3 and OH of different ROGs (as listed in Tables 2 and 3). Figure 3a displays box plots of the distributions of the fractions of total SOA produced by oxidation of these 13 compound groupings, for both O_3 and OH. Most SOA was formed as a result of terpene oxidation, which is because terpenes are highly reactive with O_3 and have

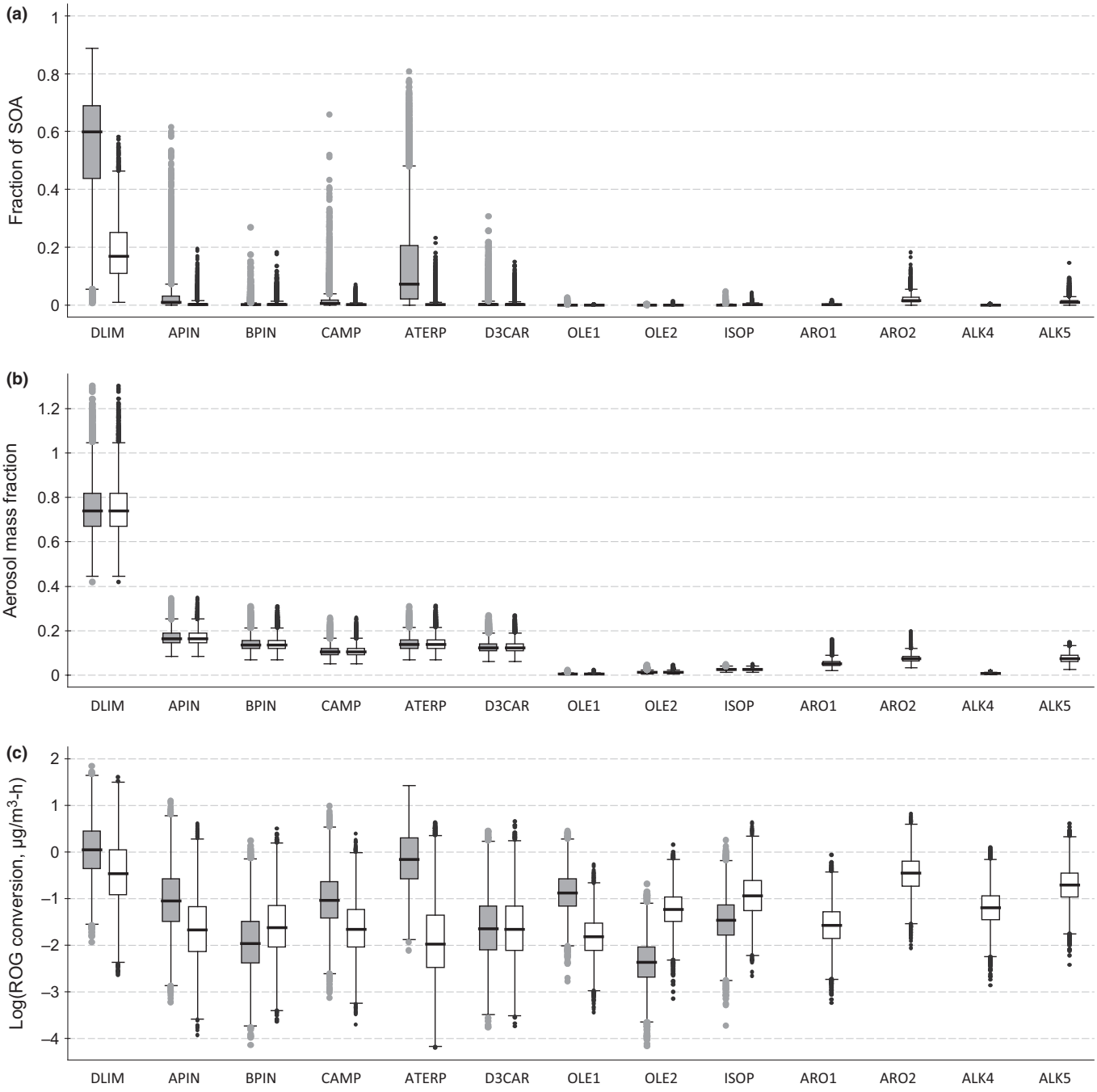

Fig. 3 Box plots summarizing the result distributions of the (a) fraction of SOA due to oxidation of each of the modeled compound classes, (b) aerosol mass fractions (AMF), and (c) log of the conversion rates for those ROG compound classes. Dark boxes are due to oxidation of compound classes by ozone and white boxes by hydroxyl radicals. See text for details

larger AMFs than other compounds, as shown in Figure 3b, which are box plots of the AMF distributions for the 13 groups. The oxidation of higher molecular weight aromatics and alkanes by OH also contributes to indoor SOA formation for a subset of the results. The potential SOA-forming impacts of OH oxidation of these classes have been largely overlooked in indoor studies, but they may be important in certain environments. Finally, for all compound groups that react with O_3, larger or at least equivalent fractional SOA was generated by O_3 rather than OH oxidation.

The specific roles of the terpenes are worth considering more, as their oxidation drives most SOA formation. Using the GM indoor mole fractions in Table 2, the terpenes comprise 8.8% of all SOA-forming compounds in this set (i.e., ones with AMFs), but they are responsible for 87% of SOA formation when summing the medians of the result distributions. The most notable terpene is d-limonene, with its oxidation by O_3 of particular importance, contributing to 44, 60, and 69% of all SOA formation at the 25th, 50th, and 75th percentiles, respectively. For SOA formation by OH

oxidation, d-limonene also contributes the most of any compound. The α-pinene was a modest contributor to SOA formation, due to its moderate AMF and indoor mole fraction, and the contribution of β-pinene was quite low, reflecting both its lower reaction rate constant and AMF. These terpenes were measured during the RIOPA campaign, and each had indoor mole fractions an order of magnitude higher than their outdoor mole fractions, illustrating the important role of indoor emissions of terpenes on indoor SOA formation.

The terpenes camphene, α-terpinene, and Δ3-carene were not measured during the RIOPA campaign. Camphene and Δ3-carene behaved similarly to α-pinene and β-pinene, respectively, but the impact of α-terpinene ozonolysis on formation deserves further discussion as it was the third largest contributor to SOA due to oxidation by either O_3 or OH. Its large role is particularly interesting as α-terpinene has an AMF similar to that of β-pinene and has an indoor mole fraction two orders of magnitude lower than d-limonene and one order lower than the other terpenes. However, α-terpinene has a reaction rate with O_3 that is one order of magnitude faster than that of d-limonene and two orders faster than the other terpenes.

To explore this, Figure 3c plots the log base-10 of the total conversion rate ($\mu g/m^3$ h) for the oxidation of all ROG classes by O_3 and OH, and it is clear that α-terpinene has a large ozonolysis conversion rate. Thus, certain ROGs with high reaction rates with indoor oxidants and low indoor mole fractions may still have large conversion rates and participate meaningfully in SOA formation indoors. As these ROGs may not be measured or regarded, they may be essentially 'stealth reactants' that have overlooked roles in certain indoor chemistry pathways. Candidates include terpinene isomers, terpinolene, α-phellandrene, and potentially terpineol isomers, which are all emitted by general purpose cleaners that are regularly used indoors (Singer et al., 2006a).

Sensitivity of SOA formation to input variables

For the sensitivity analysis, a linear regression for C_{SOA} (as well as C_{OOA}, C_{POA}, and C_{OA}) was applied, after natural log-transforming the outcome and input variables, which yielded a better fit than regressing the non-transformed variables. Input variables used were $\{\lambda, C_{O3,o}, C_{OA,o}, E_{POA}/V, \beta_{PM}, \beta_{O3}, T\}$, as well as the volume-normalized indoor emission rate for the six terpenes and outdoor mole fractions for d-limonene and α-pinene. This linear model well represented the variability in the dataset ($R^2 = 0.88$). Table 5 lists both the actual regression coefficients and standardized regression coefficients (SRC) for the linear fits. The SRC is the actual coefficient normalized by the ratio of the sample standard deviations of the dependent to independent variables. SRCs range from −1 to +1 and are useful to compare the relative importance of model inputs on the outcome: a high |SRC| indicates a large influence on the outcome, while a |SRC| near zero indicates no influence, and an input with a −SRC changes the outcome negatively and a +SRC changes the outcome positively.

The inputs that affect SOA formation positively include those related to reactant source terms. The emission rate of d-limonene (E_{DLIM}/V) had by far the largest relative influence, in either the positive or the negative direction. The outdoor O_3 mole fraction ($C_{O3,o}$) is the next but quite less influential input, followed by the emission rate of α-terpinene (E_{ATERP}/V) and then the outdoor d-limonene mole fraction ($C_{DLIM,o}$). These results again highlight the important role of d-limonene in indoor SOA formation. The fact that d-limonene has such a large role in indoor chemistry may be fortuitous as reducing the usage of products

Table 5 Actual (coefficient) and standardized regression coefficients (SRC) of natural log-transformed inputs regressed against the natural log-transformed SOA, OOA, POA, and OA predicted concentrations

	C_{SOA} ($R^2 = 0.88$)		C_{OOA} ($R^2 = 0.98$)		C_{POA} ($R^2 = 0.98$)		C_{OA} ($R^2 = 0.80$)	
Parameter	Coefficient	SRC	Coefficient	SRC	Coefficient	SRC	Coefficient	SRC
λ	−0.56	−0.31	0.51	0.60	−0.49	−0.52	−0.23	−0.32
$C_{O3,o}$	0.76	0.39	–	–	–	–	0.15	0.19
$C_{OA,o}$	0.11	0.041	1.0	0.75	–	–	0.30	0.26
E_{POA}/V	0.17	0.071	–	–	1.0	0.81	0.56	0.58
β_{PM}	−0.67	−0.15	−0.50	−0.24	−0.50	−0.22	−0.54	−0.30
β_{O3}	−0.52	−0.15	–	–	–	–	−0.088	−0.064
T	−3.8	−0.025	–	–	–	–	−0.90	−0.015
E_{DLIM}/V	0.64	0.72	–	–	–	–	0.14	0.39
E_{APIN}/V	0.033	0.045	–	–	–	–	0.0027	0.0090
E_{BPIN}/V	0.0060	0.0073	–	–	–	–	0.00050	0.0015
E_{CAMP}/V	0.0079	0.0097	–	–	–	–	−6.6E−04	−0.0020
E_{ATERP}/V	0.18	0.22	–	–	–	–	0.023	0.067
E_{D3CAR}/V	0.012	0.015	–	–	–	–	5.8E−04	0.0017
$C_{DLIM,o}$	0.15	0.091	–	–	–	–	0.020	0.030
$C_{APIN,o}$	4.6E−03	3.2E−03	–	–	–	–	9.6E−04	0.0016
Constant	19	–	−0.77	–	−0.77	–	5.2	–

in residences that contain d-limonene, such as cleaners and air fresheners (Singer et al., 2006a), is perhaps an easier task than reducing outdoor O_3, which requires a concerted effort by many stakeholders. Moreover, new consumer product formulations that do not contain d-limonene could be developed. Increases in inputs that enhance concentrations of other types of organic aerosol ($C_{OA,o}$ and E_{POA}/V) also increase SOA concentrations, but these have a low impact on SOA formation in these results.

Inputs that have a negative correlation with SOA formation include those related to reactant and product loss mechanisms. The most important driver is the air exchange rate (λ). The reduction in the air exchange rate simultaneously decreases indoor O_3 by outdoor-to-indoor transport but increases the indoor-emitted ROGs, and this increase in indoor ROG mole fractions is more influential on SOA formation than the corresponding O_3 decrease. Reducing the air exchange rate also increases the residence time of air indoors, allowing more time for SOA-forming reactions to occur. Others have noted this air exchange impact on indoor chemistry (Fadeyi et al., 2009; Waring and Siegel, 2010; Weschler and Shields, 2000). Increases in the deposition loss rates of O_3 (β_{O3}) and SOA (β_{PM}) have similar influences on SOA reduction to each other. Finally, increases in temperature (T) increase compound volatility and reduce SOA, but this effect was low relative to the other inputs, as the T range of 12°C is too small to influence SOA formation appreciably. Similarly, Warren et al. (2009) observed that SOA formation due to α-pinene oxidation changed by a factor of ~1.5 over a 12°C range.

Limitations of this approach

One important limitation of this study is that this time-averaged approach neglects SOA formation and subsequent exposure that occurs from large transient emissions of ROGs during times of high outdoor O_3. This SOA exposure could be meaningful as sizeable emissions of terpenes owing to use of consumer products, such as cleaning agents, occur in the vicinity of occupants. Relatedly, the well-mixed assumption may also cause both under- and overpredictions of exposure for occupants in different locations within the same home. Also, some indoor aerosol concentrations other than SOA are likely semivolatile in nature, and some mass might redistribute owing to indoor–outdoor temperature and available surface area differences (Weschler and Nazaroff, 2008).

Moreover, the penetration of O_3 and aerosols through the envelope is not unity (e.g., Stephens and Siegel, 2012; Stephens et al., 2011) when windows/doors are closed, and lower penetration values would reduce the indoor ozone and organic aerosol concentrations, as well as SOA formation. Regarding the O_3 and aerosol deposition rates, these would likely decrease with increasing air exchange rates (and *vice versa*) because higher air exchange rates increase air velocities and decrease transport resistance through the boundary layer (e.g., Cano-Ruiz et al., 1993). This work also assumed one PM deposition rate, which was the best estimate from the RIOPA study (Weisel et al., 2005), even though different aerosols would have different size distributions and deposit at different rates.

Finally, the inclusion of NO_x would influence the results as increasing NO_x would reduce O_3 and OH concentrations and would also generate nitrate radicals. Carslaw et al. (2012) predicted organic nitrates to dominate SOA composition in a modeling work simulating suburban UK. Interestingly, for the typical conditions in that paper, the SOA concentration was $\sim 1\ \mu g/m^3$, which is similar to this present work. The presence of NO_x also reduces the AMF for the oxidation of some compounds, for example for α-pinene (e.g., Presto and Donahue, 2006), because nitric oxide reacts strongly with peroxy radicals, competitively prohibiting the reactions of peroxy and hydroperoxyl radicals that yield low volatility, SOA-forming hydroperoxides (Kroll and Seinfeld, 2008). However, NO_x has a very small effect on SOA formation due to d-limonene ozonolysis (Zhang et al., 2006), so this AMF reduction effect is largely negligible here.

Summary

The model herein provides an expanded framework that other researchers can use to predict residential SOA formation and explore different scenarios, which includes along with it with a distribution-oriented input dataset derived from real data. The actual regression coefficients of the natural log-transformed outcomes and inputs included in Table 5 can be used for quick determinations of SOA, OOA, POA, and OA. This study has demonstrated that SOA formation can influence residential fine aerosol concentrations meaningfully in settings with certain combinations of determinants, for instance, in those with high terpene emissions and outdoor O_3 coupled with low air exchange and deposition rates. Also, results indicate that d-limonene contributes by far the most to SOA formation of any ROG, but other terpenes with high O_3 conversion rates, such as α-terpinene, should be investigated. Future studies examining SOA formation should include variations in these parameters to validate these results.

Acknowledgement

This article is based upon work supported by the National Science Foundation (Grant 1055584).

References

Arnts, R.R., Seila, R.L. and Bufalini, J.J. (1989) Determination of room temperature OH rate constants for acetylene, ethylene dichloride, ethylene dibromide, p-dichlorobenzene and carbon disulfide, *Japca*, **39**, 453–460.

Avol, E.L., Navidi, W.C. and Colome, S.D. (1998) Modeling ozone levels in and around Southern California homes, *Environ. Sci. Technol.*, **32**, 463–468.

Benning, J.L., Liu, Z., Tiwari, A., Little, J.C. and Marr, L.C. (2013) Characterizing gas-particle interactions of phthalate plasticizer emitted from vinyl flooring, *Environ. Sci. Technol.*, **47**, 2696–2703.

Bloss, C., Wagner, V., Jenkin, M.E., Volkamer, R., Bloss, W.J., Lee, J.D., Heard, D.E., Wirtz, K., Martin-Reviejo, M., Rea, G., Wenger, J.C. and Pilling, M.J. (2005) Development of a detailed chemical mechanism (MCMv3.1) for the atmospheric oxidation of aromatic hydrocarbons, *Atmos. Chem. Phys.*, **5**, 641–664.

Britigan, N., Alshawa, A. and Nizkorodov, S.A. (2006) Quantification of ozone levels in indoor environments generated by ionization and ozonolysis air purifiers, *J. Air Waste Manag. Assoc.*, **56**, 601–610.

Brown, S.K., Sim, M.R., Abramson, M.J. and Gray, C.N. (1994) Concentrations of volatile organic compounds in indoor air – A review, *Indoor Air*, **4**, 123–134.

Cano-Ruiz, J.A., Kong, D., Balas, R.B. and Nazaroff, W.W. (1993) Removal of reactive gases at indoor surfaces: combining mass transport and surface kinetics, *Atmos. Environ.*, **27A**, 2039–2050.

Carslaw, N., Mota, T., Jenkin, M.E., Barley, M.H. and McFiggans, G. (2012) A significant role for nitrate and peroxide groups on indoor secondary organic aerosol, *Environ. Sci. Technol.*, **46**, 9290–9298.

Chen, X. and Hopke, P.K. (2009) Secondary organic aerosol from α-pinene ozonolysis in dynamic chamber system, *Indoor Air*, **19**, 335–345.

Chen, X. and Hopke, P.K. (2010) A chamber study of secondary organic aerosol formation by limonene ozonolysis, *Indoor Air*, **20**, 320–328.

Chen, X., Hopke, P.K. and Carter, W.P.L. (2011) Secondary organic aerosol from ozonolysis of biogenic volatile organic compounds: chamber studies of particle and reactive oxygen species formation, *Environ. Sci. Technol.*, **45**, 276–282.

Coleman, B.K., Lunden, M.M., Destaillats, H. and Nazaroff, W.W. (2008) Secondary organic aerosol from ozone-initiated reactions with terpene-rich household products, *Atmos. Environ.*, **42**, 8234–8245.

Cupitt, L.T. (1987) *Atmospheric Persistence of Eight Air Toxics*, Research Triangle Park, NC, US Environmental Protection Agency, Office of Research and Development, Atmospheric Sciences Research Laboratory. Final report (No. PB-87-145306/XAB; EPA-600/3-87/004).

Destaillats, H., Lunden, M.M., Singer, B.C., Coleman, B.K., Hodgson, A.T., Weschler, C.J. and Nazaroff, W.W. (2006) Indoor secondary pollutants from household product emissions in the presence of ozone: a bench-scale chamber study, *Environ. Sci. Technol.*, **40**, 4421–4428.

Donahue, N.M., Robinson, A.L., Stanier, C.O. and Pandis, S.N. (2006) Coupled partitioning, dilution, and chemical aging of semivolatile organics, *Environ. Sci. Technol.*, **40**, 2635–2643.

El Orch, Z., Stephens, B. and Waring, M.S. (2014) Predictions and determinants of size-resolved particle infiltration factors in single-family homes in the U.S., *Build. Environ.* http://dx.doi.org/10.1016/j.buildenv.2014.01.006.

Fadeyi, M.O., Weschler, C.J. and Tham, K.W. (2009) The impact of recirculation, ventilation and filters on secondary organic aerosols generated by indoor chemistry, *Atmos. Environ.*, **43**, 3538–3547.

Fadeyi, M.O., Weschler, C.J., Tham, K.W., Wu, W.Y. and Sultan, Z.M. (2013) Impact of human presence on secondary organic aerosols derived from ozone-initiated chemistry in a simulated office environment, *Environ. Sci. Technol.*, **47**, 3933–3941.

Gierczak, T., Gilles, M.K., Bauerle, S. and Ravishankara, A.R. (2003) Reaction of hydroxyl radical with acetone. 1. Kinetics of the reactions of OH, OD, and 18OH with acetone and acetone-d 6, *J. Phys. Chem. A*, **107**, 5014–5020.

Griffin, R.J., Cocker, D.R., Flagan, R.C. and Seinfeld, J.H. (1999) Organic aerosol formation from the oxidation of biogenic hydrocarbons, *J. Geophys. Res.*, **104**, 3555–3567.

Hoffmann, T., Odum, J.R., Bowman, F. and Collins, D. (1997) Formation of organic aerosols from the oxidation of biogenic hydrocarbons, *J. Atmos. Chem.*, **26**, 189–222.

Hubbard, H.F., Coleman, B.K., Sarwar, G. and Corsi, R.L. (2005) The effects of an ozone generating air purifier on indoor secondary particles in three residential dwellings, *Indoor Air*, **15**, 432–444.

Jenkin, M.E., Saunders, S.M. and Pilling, M.J. (1997) The tropospheric degradation of volatile organic compounds: a protocol for mechanism development, *Atmos. Environ.*, **31**, 81–104.

Jenkin, M.E., Saunders, S.M., Wagner, V. and Pilling, M.J. (2003) Protocol for the development of the Master Chemical Mechanism, MCM v3 (Part B): tropospheric degradation of aromatic volatile organic compounds, *Atmos. Chem. Phys.*, **3**, 181–193.

Klepeis, N.E., Nelson, W.C., Ott, W.R., Robinson, J.P., Tsang, A.M., Switzer, P., Behar, J.V., Hern, S.C. and Engelmann, W.H. (2001) The national human activity pattern survey (NHAPS): a resource for assessing exposure to environmental pollutants, *J. Expo. Anal. Environ. Epidemiol.*, **11**, 231–252.

Kroll, J.H. and Seinfeld, J.H. (2008) Chemistry of secondary organic aerosol: formation and evolution of low-volatility organics in the atmosphere, *Atmos. Environ.*, **42**, 3593–3624.

Lane, T.E., Donahue, N.M. and Pandis, S.N. (2008) Simulating secondary organic aerosol formation using the volatility basis-set approach in a chemical transport model, *Atmos. Environ.*, **42**, 7439–7451.

Lee, K., Vallarino, J., Dumyahn, T., Ozkaynak, H. and Spengler, J.D. (1999) Ozone decay rates in residences, *J. Air Waste Manag. Assoc.*, **49**, 1238–1244.

Lee, S.C., Lam, S. and Kin Fai, H. (2001) Characterization of VOCs, ozone, and PM10 emissions from office equipment in an environmental chamber, *Build. Environ.*, **36**, 837–842.

Liu, C., Morrison, G.C. and Zhang, Y. (2012) Role of aerosols in enhancing SVOC flux between air and indoor surfaces and its influence on exposure, *Atmos. Environ.*, **55**, 347–356.

Logue, J.M., McKone, T.E., Sherman, M.H. and Singer, B.C. (2011) Hazard assessment of chemical air contaminants measured in residences, *Indoor Air*, **21**, 92–109.

Morrison, G., Shaughnessy, R. and Shu, S. (2011) Setting maximum emission rates from ozone emitting consumer appliances in the United States and Canada, *Atmos. Environ.*, **45**, 2009–2016.

Niu, J., Thomas, C.W. and Tung, J.B. (2001) Ozone emission rate testing and ranking method using environmental chamber, *Atmos. Environ.*, **35**, 2143–2151.

Odum, J.R., Hoffmann, T., Bowman, F., Collins, D., Flagan, R.C. and Seinfeld, J.H. (1996) Gas/particle partitioning and secondary organic aerosol yields, *Environ. Sci. Technol.*, **30**, 2580–2585.

Odum, J.R., Jungkamp, T.P.W., Griffin, R.J., Flagan, R.C. and Seinfeld, J.H. (1997) The atmospheric aerosol-forming potential of whole gasoline vapor, *Science*, **276**, 96–99.

Plum, C.N., Sanhueza, E., Atkinson, R., Carter, W.P. and Pitts, J.N. (1983) Hydroxyl radical rate constants and photolysis rates of alpha-dicarbonyls, *Environ. Sci. Technol.*, **17**, 479–484.

Polidori, A., Turpin, B.J., Lim, H., Cabada, J.C., Subramanian, R., Pandis, S.N. and Robinson, A.L. (2006a) Local and regional secondary organic aerosol: insights from a year of semi-continuous carbon measurements at Pittsburgh, *Aerosol Sci. Tech.*, **40**, 861–872.

Polidori, A., Turpin, B., Meng, Q.Y., Lee, J.H., Weisel, C., Morandi, M., Colome, S., Stock, T., Winer, A., Zhang, J., Kwon, J., Alimokhtari, S., Shendell, D., Jones, J., Farrar, C. and Maberti, S. (2006b) Fine organic particulate matter dominates indoor-generated PM2.5 in RIOPA homes, *J. Expo. Sci. Environ. Epidemiol.*, **16**, 321–331.

Pope, C.A. and Dockery, D.W. (2006) Health effects of fine particulate air pollution: lines that connect, *J. Air Waste Manag. Assoc.*, **56**, 709–742.

Presto, A.A. and Donahue, N.M. (2006) Investigation of α-pinene + ozone secondary organic aerosol formation at low total aerosol mass, *Environ. Sci. Technol.*, **40**, 3536–3543.

Riley, W.J., Mckone, T.E., Lai, A.C.K. and Nazaroff, W.W. (2002) Indoor particulate matter of outdoor origin: importance of size-dependent removal mechanisms, *Environ. Sci. Technol.*, **36**, 200–207.

Rohr, A.C. (2013) The health significance of gas-and particle-phase terpene oxidation products: a review, *Environ. Int.*, **60**, 145–162.

Sabersky, R.H., Sinema, D.A. and Shair, F.H. (1973) Concentrations, decay rates, and removal of ozone and their relation to establishing clean indoor air, *Environ. Sci. Technol.*, **7**, 347–353.

Sarnat, J.A., Brown, K.W., Schwartz, J., Coull, B.A. and Koutrakis, P. (2005) Ambient gas concentrations and personal particulate matter exposures: implications for studying the health effects of particles, *Epidemiology*, **16**, 385–395.

Sarwar, G. and Corsi, R. (2007) The effects of ozone/limonene reactions on indoor secondary organic aerosols, *Atmos. Environ.*, **41**, 959–973.

Sarwar, G., Corsi, R., Kimura, Y., Allen, D. and Weschler, C.J. (2002) Hydroxyl radicals in indoor environments, *Atmos. Environ.*, **36**, 3973–3988.

Sarwar, G., Corsi, R., Allen, D. and Weschler, C. (2003) The significance of secondary organic aerosol formation and growth in buildings: experimental and computational evidence, *Atmos. Environ.*, **37**, 1365–1381.

Saunders, S.M., Jenkin, M.E., Derwent, R.G. and Pilling, M.J. (2003) Protocol for the development of the Master Chemical Mechanism, MCM v3 (Part A): tropospheric degradation of non-aromatic volatile organic compounds, *Atmos. Chem. Phys.*, **3**, 161–180.

Singer, B.C., Destaillats, H., Hodgson, A.T. and Nazaroff, W.W. (2006a) Cleaning products and air fresheners: emissions and resulting concentrations of glycol ethers and terpenoids, *Indoor Air*, **16**, 179–191.

Singer, B.C., Coleman, B.K., Destaillats, H., Hodgson, A.T., Lunden, M.M., Weschler, C.J. and Nazaroff, W.W. (2006b) Indoor secondary pollutants from cleaning product and air freshener use in the presence of ozone, *Atmos. Environ.*, **40**, 6696–6710.

Stephens, B. and Siegel, J.A. (2012) Penetration of ambient submicron particles into single-family residences and associations with building characteristics, *Indoor Air*, **22**, 501–513.

Stephens, B., Gall, E.T. and Siegel, J.A. (2011) Measuring the penetration of ambient ozone into residential buildings, *Environ. Sci. Technol.*, **46**, 929–936.

Tung, T.C.W., Niu, J., Burnett, J. and Hung, K. (2005) Determination of ozone emission from a domestic air cleaner and decay parameters using environmental chamber tests, *Indoor Built Environ.*, **14**, 29–37.

Turpin, B.J., Weisel, C.P., Morandi, M., Colome, S., Stock, T., Eisenreich, S. and Buckley, B. (2007) *Relationships of Indoor, Outdoor, and Personal Air (RIOPA): Part II. Analyses of Concentrations of Particulate Matter Species*. HEI Research Report 130; NUATRC Research Report 10. Boston, MA, Health Effects Institute, and Houston, TX, Mickey Leland National Urban Air Toxics Research Center.

USEPA. (2006) *Ozone Population Exposure Analysis for Selected Urban Areas*, Research Triangle Park, NC, US Environmental Protection Agency.

Wainman, T., Zhang, J., Weschler, C.J. and Lioy, P.J. (2000) Ozone and limonene in indoor air: a source of submicron particle exposure, *Environ. Health Perspect.*, **108**, 1139–1145.

Wallace, L. (1996) Indoor particles: a review, *J. Air Waste Manag. Assoc.*, **46**, 98–126.

Wallace, L. (2006) Indoor sources of ultrafine and accumulation mode particles: size distributions, size-resolved concentrations, and source strengths, *Aerosol Sci. Technol.*, **40**, 348–360.

Wang, C. and Waring, M.S. (2014) Secondary organic aerosol formation initiated from reactions between ozone and surface-sorbed squalene, *Atmos. Environ.*, **84**, 222–229.

Waring, M.S. and Siegel, J.A. (2010) The influence of HVAC systems on indoor secondary organic aerosol formation, *ASHRAE Trans.*, **116**, 556–571.

Waring, M.S. and Siegel, J.A. (2013) Indoor secondary organic aerosol formation initiated from reactions between ozone and surface-sorbed d-limonene, *Environ. Sci. Technol.*, **47**, 6341–6348.

Waring, M.S., Siegel, J.A. and Corsi, R.L. (2008) Ultrafine particle removal and generation by portable air cleaners, *Atmos. Environ.*, **42**, 5003–5014.

Waring, M.S., Wells, J.R. and Siegel, J.A. (2011) Secondary organic aerosol formation from ozone reactions with single terpenoids and terpenoid mixtures, *Atmos. Environ.*, **45**, 4235–4242.

Warren, B., Austin, R.L. and Cocker, D.R. III (2009) Temperature dependence of secondary organic aerosol, *Atmos. Environ.*, **43**, 3548–3555.

Weisel, C.P., Zhang, J., Turpin, B.J., Morandi, M.T., Colome, S., Stock, T.H., Spektor, D.M., Korn, L, Winer, A.M., Kwon, J., Meng, Q.Y., Zhang, L., Harrington, R., Liu, W., Reff, A., Lee, J.H., Alimokhtari, S., Mohan, K., Shendell, D., Jones, J., Farrar, L., Maberti, S. and Fan, T. (2005) *Relationships of Indoor, Outdoor, and Personal Air (RIOPA): Part I. Collection Methods and Descriptive Analyses*. HEI Research Report 130; NUATRC Research Report 7. Boston MA, Health Effects Institute; Houston TX, Mickey Leland National Urban Air Toxics Research Center.

Weschler, C.J. (2000) Ozone in indoor environments: concentration and chemistry, *Indoor Air*, **10**, 269–288.

Weschler, C.J. (2006) Ozone's impact on public health: contributions from indoor exposures to ozone and products of ozone-initiated chemistry, *Environ. Health Perspect.*, **114**, 1489.

Weschler, C.J. and Nazaroff, W.W. (2008) Semivolatile organic compounds in indoor environments, *Atmos. Environ.*, **42**, 9018–9040.

Weschler, C.J. and Shields, H.C. (1996) Production of hydroxyl radical in indoor air, *Environ. Sci. Technol.*, **30**, 3250–3258.

Weschler, C.J. and Shields, H.C. (1997) Measurements of the hydroxyl radical in a manipulated but realistic indoor environment, *Environ. Sci. Technol.*, **31**, 3719–3722.

Weschler, C.J. and Shields, H.C. (1999) Indoor ozone/terpene reactions as a source of indoor particles, *Atmos. Environ.*, **33**, 2301–2312.

Weschler, C.J. and Shields, H.C. (2000) The influence of ventilation on reactions among indoor pollutants: modeling and experimental observations, *Indoor Air*, **10**, 92–100.

Wolkoff, P., Clausen, P.A., Larsen, K., Hammer, M., Larsen, S.T. and Nielsen, G.D. (2008) Acute airway effects of ozone-initiated d-limonene chemistry: importance of gaseous products, *Toxicol. Lett.*, **181**, 171–176.

Wu, P., Li, J., Li, S. and Tao, F.M. (2012) Theoretical study of mechanism and kinetics for the addition of hydroxyl radi-

cal to phenol, *Sci. China Chem.*, **55**, 270–276.

Youssefi, S. and Waring, M.S. (2012) Predicting secondary organic aerosol formation from terpenoid ozonolysis with varying yields in indoor environments, *Indoor Air*, **22**, 415–426.

Zhang, J., Hartz, K.E.H., Pandis, S.N. and Donahue, N.M. (2006) Secondary organic aerosol formation from limonene ozonolysis: homogeneous and heterogeneous influences as a function of NOx, *J. Phys. Chem. A*, **110**, 11053–11063.

Zuraimi, M.S., Weschler, C.J., Tham, K.W. and Fadeyi, M.O. (2007) The impact of building recirculation rates on secondary organic aerosols generated by indoor chemistry, *Atmos. Environ.*, **41**, 5213–5223.